

Physics 4P06:  
Reversing Interfaces in the Nonlinear Diffusion  
Equation

Peter Gysbers<sup>‡</sup>

Supervisors: J. M. Foster<sup>†</sup> & D. E. Pelinovsky<sup>†</sup>

<sup>‡</sup>Department of Physics and Astronomy, <sup>†</sup>Department of Mathematics and Statistics,  
McMaster University, Hamilton, Ontario, Canada

April 19, 2016

**Abstract**

A variety of natural phenomena are described by a nonlinear diffusion equation with an absorption term. In this report self-similar solutions to the nonlinear diffusion equation are constructed for reversing interfaces. The asymptotic behaviours of the solution for small and large concentrations are determined through a method of invariant manifolds and then connected numerically. Bifurcation diagrams are offered and justified with a Schrödinger equation equivalent to a 3-dimensional isotropic harmonic oscillator.

# 1 Introduction

The slow diffusion equation with absorption describes a variety of physical processes including: the spread of thin viscous films with evaporation [1], dispersion of biological populations with a death rate [7], nonlinear heat conduction with heat loss [8] and fluid flows in porous media with drainage [2]. Here it takes the following form

$$\frac{\partial h}{\partial t} = \frac{\partial}{\partial x} \left( h^m \frac{\partial h}{\partial x} \right) - h^n \quad (1.1)$$

where  $h$  is a positive function with compact support. The dependent variable  $h$  represents a concentration or temperature while  $x$  and  $t$  denote space and time respectively. This form describes a family of equations each with different values of  $m$  and  $n$  in the exponents. The parameters  $m$  and  $n$  are restricted to the ranges  $m > 0$  and  $n < 1$  corresponding to slow diffusion and strong absorption respectively. The exponents are further limited by a technical constraint  $m + n > 1$  which emerges later (equation (1.8)) to ensure the desired dynamics.

Interfaces correspond to the points on the  $x$ -axis where positive solutions  $h$  meet regions where  $h$  is identically zero. Slow diffusion ( $m > 0$ ) enforces that the interfaces move at a finite speed [8] and strong absorption ( $n < 1$ ) ensures finite-time extinction [9, 10] i.e. the solution eventually vanishes with  $h = 0$  everywhere. The initial shape of  $h$  and the values of  $m$  and  $n$  will determine the behaviour of the interface. The interface may have one of several behaviours: (i) the interface will recede monotonically until the solution vanishes completely, (ii) the interface will initially advance then reverse its behaviour and recede, or (iii) more complicated behaviour with multiple instances of advancing and receding motion.

Denoting the location of the left interface by  $x = \ell(t)$ , the behaviour of the interface is described as “reversing” if  $\dot{\ell} < 0$  before reversing time and  $\dot{\ell} > 0$  after reversing time (a dot denotes differentiation with respect to time). The term “anti-reversing” describes the opposite scenario. This report seeks to construct a self-similar solution of  $h$  in which the interface exhibits reversing or anti-reversing behaviour.

The boundary conditions on (1.1) are the conditions that  $h$  must be continuous at the interface  $h|_{x=\ell(t)} = 0$  and that the flux of  $h$  through the interface is zero. The zero flux condition is written [5]:

$$\dot{\ell} = -h^{m-1} \frac{\partial h}{\partial x} \Big|_{x=\ell(t)} + \left( (1-n) \frac{\partial}{\partial x} (h^n) \Big|_{x=\ell(t)} \right)^{-1}$$

A self-similar solution of equation (1.1) captures the relevant dynamics of reversing interfaces. Placing the location and time of a reversing event at the origin of space and time,

reversing interfaces can be described with the self-similar reduction [6]:

$$h(x, t) = (\pm t)^{\frac{1}{1-n}} H_{\pm}(\xi), \quad \xi = x(\pm t)^{-\frac{m+1-n}{2(1-n)}}, \quad \pm t > 0 \quad (1.2)$$

The pair of functions  $H_+$  and  $H_-$  must then be found from the following equations:

$$\frac{d}{d\xi} \left( H_{\pm}^m \frac{dH_{\pm}}{d\xi} \right) \pm \frac{m+1-n}{2(1-n)} \xi \frac{dH_{\pm}}{d\xi} = H_{\pm}^n \pm \frac{1}{1-n} H_{\pm} \quad (1.3)$$

The required solutions are positive functions on the semi-infinite line  $[A_{\pm}, \infty)$  that satisfy:

$$(i) : H_{\pm}(\xi) \rightarrow 0 \text{ as } \xi \rightarrow A_{\pm} \quad (1.4)$$

$$(ii) : H_{\pm}(\xi) \text{ is monotonically increasing for all } \xi > A_{\pm} \quad (1.5)$$

$$(iii) : H_{\pm}(\xi) \rightarrow +\infty \text{ as } \xi \rightarrow +\infty \quad (1.6)$$

In addition, continuity of  $h$  at  $t = 0$  means that  $H_+$  and  $H_-$  must be matched in the far-field of  $\xi$ , i.e.

$$\lim_{\xi \rightarrow \infty} \frac{H_+(\xi)}{H_-(\xi)} = 1 \quad (1.7)$$

Each solution to (1.1), made of a matching pair of functions  $H_+$  and  $H_-$ , will have a corresponding pair of values  $A_+$  and  $A_-$  for which the interface will exhibit reversing ( $A_{\pm} > 0$ ) or anti-reversing behaviour ( $A_{\pm} < 0$ ).

The solutions of this form imply the following behaviour for the interface [4]:

$$\ell(t) = A_{\pm} (\pm t)^{\frac{m+1-n}{2(1-n)}} \quad (1.8)$$

Reversing behaviour requires the  $\dot{\ell}(t)|_{t=0} = 0$  and so (1.8) implies  $\frac{m+1-n}{2(1-n)} > 1$ , which is equivalent to the constraint  $m+n > 1$  discussed earlier.

The case when  $A_{\pm} = 0$  has an exact solution:

$$H_0(\xi) = \left( \frac{\xi}{x_Q} \right)^{\frac{2}{m+1-n}}, \quad x_Q^2 = \frac{2(m+1+n)}{(m+1-n)^2}, \quad (1.9)$$

which corresponds to a stationary solution of (1.1) with  $h(x, t) = h(x) = \left( \frac{x}{x_Q} \right)^{\frac{2}{m+1-n}}$ .

Solutions which exhibit reversing or anti-reversing behaviours with  $A_{\pm} \neq 0$  need to be found numerically. Preliminary results for the case  $n = 0$  were developed in [3]. This report extends the method and results for all  $n > 1 - m$ . The numerical procedure to produce solutions is generated using a dynamical system framework in §2 which can be used to rigorously justify asymptotic behaviours. The numerical results will be covered in §3.

Bifurcations of solutions with  $A_{\pm} \neq 0$  from the stationary solution (1.9) are studied in §4.

## 2 Invariant Manifolds

This section describes the dynamical systems framework which will be used later (in §3) to construct solutions numerically.

### 2.1 Near-Field

For small values of  $H_{\pm}$  the scalar equation (1.3) can be written as a vector system with the variables  $u = H_{\pm}$  and  $w = H_{\pm}^m \frac{dH_{\pm}}{d\xi}$ .

$$\begin{aligned}\frac{du}{d\xi} &= \frac{w}{u^m} \\ \frac{dw}{d\xi} &= u^n \pm \frac{u}{1-n} \mp \frac{m+1-n}{2(1-n)} \xi \frac{w}{u^m}\end{aligned}$$

The interface is located at  $\xi = A$  but at this point  $u = 0$  resulting in a singularity. The way around this is to use a parametrization with a new variable  $\tau$  such that

$$\frac{d\xi}{d\tau} = u^m \quad \text{with} \quad \xi \rightarrow A \quad \text{as} \quad \tau \rightarrow -\infty$$

Denoting a derivative with respect to  $\tau$  with a dot, the following dynamical system is obtained:

$$\begin{aligned}\dot{\xi} &= u^m \\ \dot{u} &= w \\ \dot{w} &= u^m \left( u^n \pm \frac{u}{1-n} \right) \mp \frac{m+1-n}{2(1-n)} \xi w\end{aligned}\tag{2.1}$$

The family of equilibrium points for this system is given by  $(\xi, u, w) = (A, 0, 0)$  with  $A \in \mathbb{R}$  an arbitrary parameter. Each equilibrium point is associated with the Jacobian matrix

$$\begin{bmatrix} 0 & mu^{m-1} & 0 \\ 0 & 0 & 1 \\ \mp \frac{m+1-n}{2(1-n)} & (m+n)u^{m+n-1} \pm \frac{1+m}{1-n}u^m & \mp \frac{m+1-n}{2(1-n)}\xi \end{bmatrix} \Big|_{(A,0,0)} = \begin{bmatrix} 0 & 0 & 0 \\ 0 & 0 & 1 \\ 0 & 0 & \mp \frac{m+1-n}{2(1-n)}A \end{bmatrix}$$

This matrix has a double zero eigenvalue and a nonzero eigenvalue  $\pm \frac{m+1-n}{2(1-n)}A$ , if  $A \neq 0$ .

The linearization of the dynamical system therefore has a two-dimensional center manifold and a one-dimensional stable ( $\pm A > 0$ ) or unstable ( $\pm A < 0$ ) manifold. A trajectory corresponding to a viable solution must leave the equilibrium point as  $\tau$  increases.

For  $\pm A > 0$  the escaping trajectory must belong to the center manifold  $W_c$ . This manifold is parametrized by  $(\xi, u)$  near  $(A, 0)$  while

$$w = \frac{2(1-n)}{(m+1-n)A} u^{m+n} + \dots \quad (2.2)$$

Dynamics of the system on the center manifold  $W_c$  is topologically equivalent to the dynamics of the two-dimensional system

$$\begin{cases} \dot{\xi} = u^m \\ \dot{u} = \pm \frac{2u^m}{(m+1)A} \end{cases}$$

For every  $\pm A > 0$ , there exists exactly one trajectory on  $W_c$ , which approaches the equilibrium point  $(A, 0, 0)$  as  $\tau \rightarrow -\infty$  if  $\pm A > 0$ .

For  $\pm A < 0$ , the trajectory leaving the equilibrium point belongs to the unstable manifold  $W_u$ . This manifold is parametrized by  $u$  near 0 while

$$\begin{aligned} \xi &= A \mp \frac{2(1-n)}{m(m+1-n)A} u^m + \dots \\ w &= \mp \frac{m+1-n}{2(1-n)} Au + \dots \end{aligned} \quad (2.3)$$

Dynamics of the system on the unstable manifold  $W_u$  is topologically equivalent to dynamics of the linear equation

$$\dot{u} = \mp \frac{m+1-n}{2(1-n)} Au .$$

## 2.2 Far-Field

Trajectories departing from the equilibrium point are expected to arrive at infinite values of  $\xi$  and  $u$ . To study behaviour in the far-field a transformation to variables  $(x, y, z)$  is used such that an infinite value of  $u$  maps to a zero value of  $y$ . The following transformation works:

$$\xi = \frac{x}{y^{\frac{m+1-n}{2(1-n)}}}, \quad u = \frac{1}{y^{\frac{1}{1-n}}}, \quad w = \frac{z}{y^{\frac{m+3-n}{2(1-n)}}} .$$

This results in a singularity in the derivatives with respect to  $\tau$  and so another parametrization to the new variable  $s$  can be used such that

$$\frac{d\tau}{ds} = y^{\frac{m+1-n}{2(1-n)}} \quad \text{with} \quad y \rightarrow 0 \quad \text{as} \quad s \rightarrow +\infty .$$

A new dynamical system is obtained (denoting a derivative with respect to  $s$  with a prime)

$$\begin{aligned} x' &= y - \left( \frac{m+1-n}{2} \right) xz \\ y' &= -(1-n)yz \\ z' &= y^2 \pm \left( \frac{1}{1-n} \right) y \mp \left( \frac{m+1-n}{2(1-n)} \right) xz - \left( \frac{m+3-n}{2} \right) z^2 \end{aligned} \tag{2.4}$$

The family of equilibrium points for this system is given by  $(x, y, z) = (x_0, 0, 0)$  with  $x_0 \in \mathbb{R}$  an arbitrary parameter. Each equilibrium point is associated with the Jacobian matrix

$$\begin{aligned} & \begin{bmatrix} -\left(\frac{m+1-n}{2}\right)z & 1 & -\left(\frac{m+1-n}{2}\right)x \\ 0 & -(1-n)z & -(1-n)y \\ \mp\left(\frac{m+1-n}{2(1-n)}\right)z & 2y \pm \left(\frac{1}{1-n}\right)y & \mp\left(\frac{m+1-n}{2(1-n)}\right)x - (m+3-n)z \end{bmatrix} \Big|_{(x_0, 0, 0)} \\ &= \begin{bmatrix} 0 & 1 & -\left(\frac{m+1-n}{2}\right)x_0 \\ 0 & 0 & 0 \\ 0 & \pm\frac{1}{1-n} & \mp\left(\frac{m+1-n}{2(1-n)}\right)x_0 \end{bmatrix} \end{aligned}$$

This matrix has a double zero eigenvalue and a simple eigenvalue  $\mp\left(\frac{m+1-n}{2(1-n)}\right)x_0$ , if  $x_0 \neq 0$ . Relevant trajectories in the system require  $x_0 > 0$ . If  $x_0 > 0$ , the linearization of the system therefore has a two-dimensional center manifold and a one-dimensional stable or unstable manifold depending on the upper or lower sign.

The center manifold  $W_c$  is parametrized by  $(x, z)$  near  $(x_0, 0)$  while

$$y = \frac{m+1-n}{2} \left[ xz \pm (1-n) \left( 1 - \frac{m+1-n}{2} x_0^2 \right) z^2 \right] + \dots \tag{2.5}$$

The dynamics of the system on the center manifold  $W_c$  is topologically equivalent to the

dynamics in the two-dimensional linear system

$$\begin{cases} x' = \pm(1-n) \left(\frac{m+1-n}{2}\right) \left(1 - \frac{m+1-n}{2}x_0^2\right) z^2 \\ z' = -z^2 \end{cases} \quad (2.6)$$

There exists exactly one trajectory on  $W_c$  which approaches the equilibrium  $(x_0, 0, 0)$  as  $s \rightarrow +\infty$ .

### 3 Numerical Results

This section describes the numerical approach which is used to find solutions for  $H_+$  and  $H_-$  by connecting behaviours of the near-field and far-field systems.

#### 3.1 Solutions for $H_-$ ( $t < 0$ )

A solution of (1.3) before reversing can be constructed numerically as a trajectory from infinite to finite values of  $H_-$ . This can be done by integrating the system (2.4) from the equilibrium point  $(x_0, 0, 0)$  in the far-field towards the equilibrium point  $(A_-, 0, 0)$  of the system (2.1) in the near-field. This is done via the following numerical procedure:

1. Select a value of  $x_0 > 0$ . The trajectory would then follow an integration of (2.4) backward in the value  $s$ . However since  $(x_0, 0, 0)$  is an equilibrium point, starting at exactly  $x = x_0$  is poor choice as the trajectory will not escape the equilibrium point. The solution is to take a small step  $\delta \ll 1$  away from  $(x_0, 0, 0)$  in the  $z$  direction and use asymptotic behaviour along the center manifold (2.5) to determine the initial values of  $x$  and  $y$ :

$$\begin{cases} x = x_0 + (1-n) \left(\frac{m+1-n}{2}\right) \left(1 - \frac{m+1-n}{2}x_0^2\right) \delta \\ y = \left(\frac{m+1-n}{2}\right) x_0 \delta \\ z = \delta \end{cases}$$

With these initial conditions the system can be integrated with decreasing values of  $s$ . As in [3] the integration was carried out with the `ode45` routine in MATLAB using choosing  $\delta \in (10^{-3}, 10^{-2})$ .

2. Physically relevant trajectories must reach some point  $(\xi, u, w) = (A_-, 0, 0)$  in the near field. For accurate integration in the near-field a switch of variables is required so the integration can be continued with the near-field system (2.1) with decreasing  $\tau$ . The conditions for when this switch occurs is fairly arbitrary. Here, a value of  $xy^{-\frac{m+1-n}{2(1-n)}} = \xi = 20$  was used, in the same fashion as [3]. The MATLAB `Events` function was used to automate

stopping integration, saving the current  $(x, y, z)$  values, converting them to  $(\xi, u, w)$  values then starting integration of the near-field system. The near-field system was integrated with the `ode15s` routine.

3. Not all  $x_0$  values will result in trajectories that reach the near field equilibrium point but trajectories must reach either the  $u = 0$  or  $w = 0$  plane. If for two trajectories corresponding to different selected values of  $x_0$ , one crosses  $u = 0$  and the other  $w = 0$  then there must exist an intermediate value of  $x_0$  for which the trajectory reaches a point where both  $u = 0$  and  $w = 0$ . To find this  $x_0$  value a bisection algorithm was constructed to narrow down the range of desired  $x_0$  values to arbitrary accuracy (machine precision). The `Events` function was again used to detect if either  $u = 0$  or  $w = 0$  occurred causing the integration to stop and recording the final values of either  $(\xi, u)$  or  $(\xi, w)$  choosing the non-zero element of  $(u, w)$ .

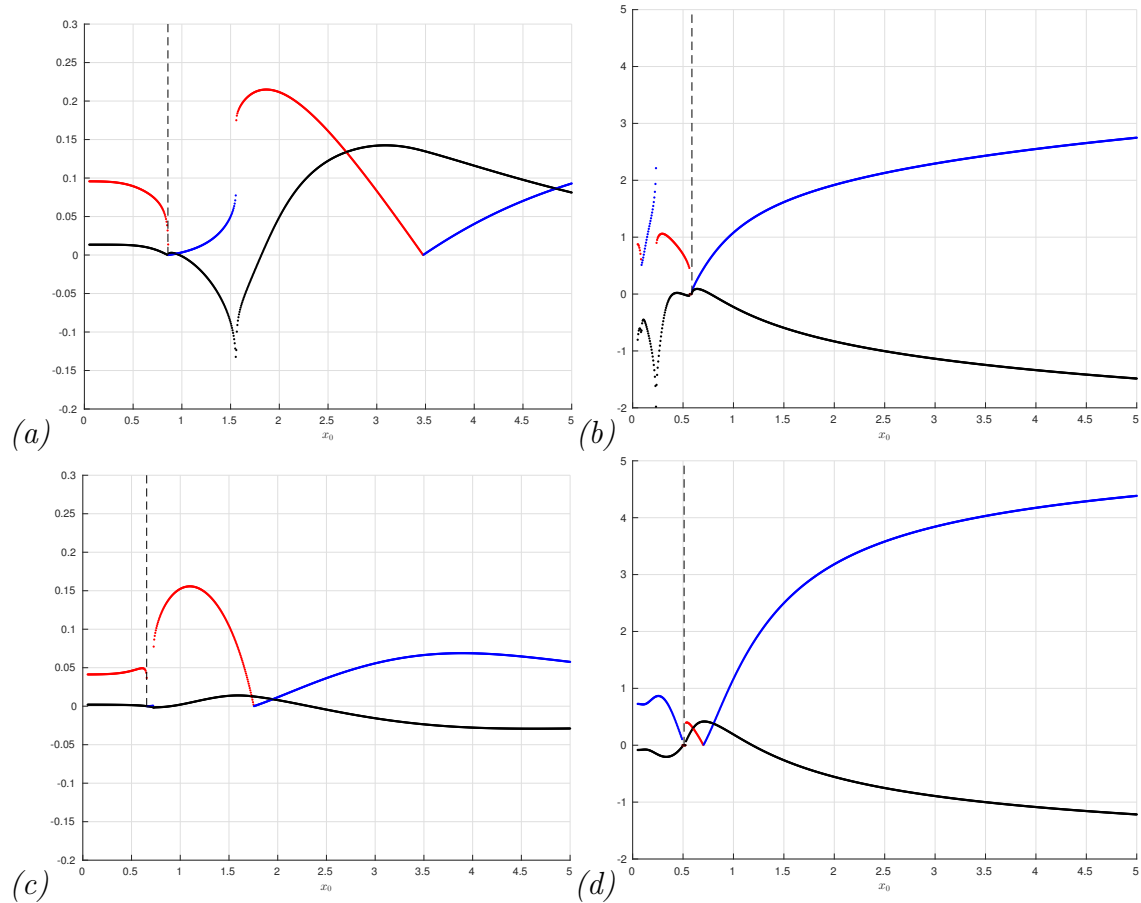


Figure 3.1: (a)  $m = 3, n = +1/2$ , (b)  $m = 3, n = -1/2$ , (c)  $m = 5, n = +1/2$ , (d)  $m = 5, n = -1/2$ . The blue, red, and black curves show the value of  $w$  at  $u = 0$ , the value of  $u$  at  $w = 0$ , and the value of  $\xi$  at the termination point respectively. The dashed vertical line marks the location of  $x_Q$ .



The non-trivial solutions for  $H_-$  correspond to trajectories with particular initial values  $x_0 = x_0^*$  which reach  $(A_-, 0, 0)$  for some finite  $A_- \neq 0$ . Trivial solutions which reach  $\xi = A_- = 0$  correspond to  $x_0^* = x_Q = \sqrt{2(m+1+n)}/(m+1-n)$  and the stationary solution of (1.3). So by selecting a reasonable range of  $x_0$  values containing  $x_Q$  the numerical scheme is guaranteed to find at least one value  $x_0^*$  for all values of  $m > 1, n < 1, m+n > 1$ . Representative plots of the resulting final  $\xi, u$  or  $w$  values for a range of initial  $x_0$  values and a range of  $m$  and  $n$  values are found in Figure 3.1. The crossing point of trajectory through the zero of the  $y$ -axis corresponds to a value of  $x_0^*$ .

As seen in Figure 3.1 the behaviour of trajectories in the near-field is different between solutions with  $A_- < 0$  and  $A_- > 0$ . For  $A_- < 0$  obtaining a high accuracy value of  $A_-$  is more difficult and an extrapolation procedure is used to estimate its value.

The found  $x_0^*$  values are plotted against  $m$  for different values of  $n$  in Figure 3.2. It can be seen that in addition to the trivial solution there are many other solutions. The colour of points on this plot indicates the sign of  $A_-$ , typical values of  $A_-$  along a curve in Figure 3.2 are plotted against  $m$  in Figure 3.3. Another noteworthy feature of Figure 3.2 are the additional branches of solutions that depart from the  $x_0 = x_Q$  branch at each value of  $m = (1-n)(2k-1)$  for  $k \in \mathbb{N}$ . The appearance of these branches is justified in §4.

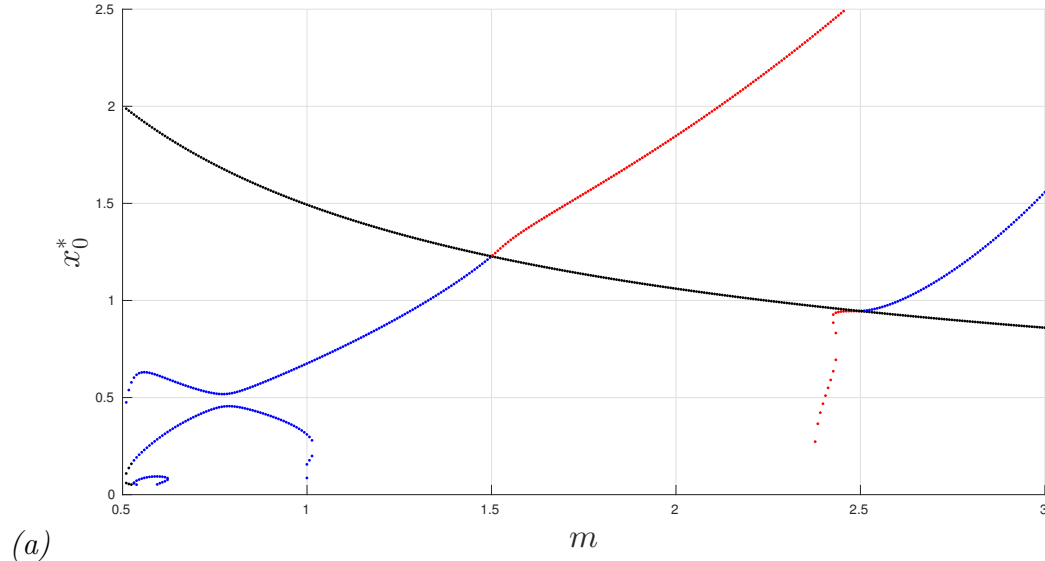


Figure 3.2: *The variation of  $x_0^*$  versus  $m$  for different values of  $n$ : (a)  $n = 1/2$ , (b)  $n = 0$ , (c)  $n = -1/2$  and (d)  $n = -1$ . The black points correspond to the stationary solution (1.9) while points in red or blue correspond to  $A_- > 0$  and  $A_- < 0$  respectively. (Continued on next page)*

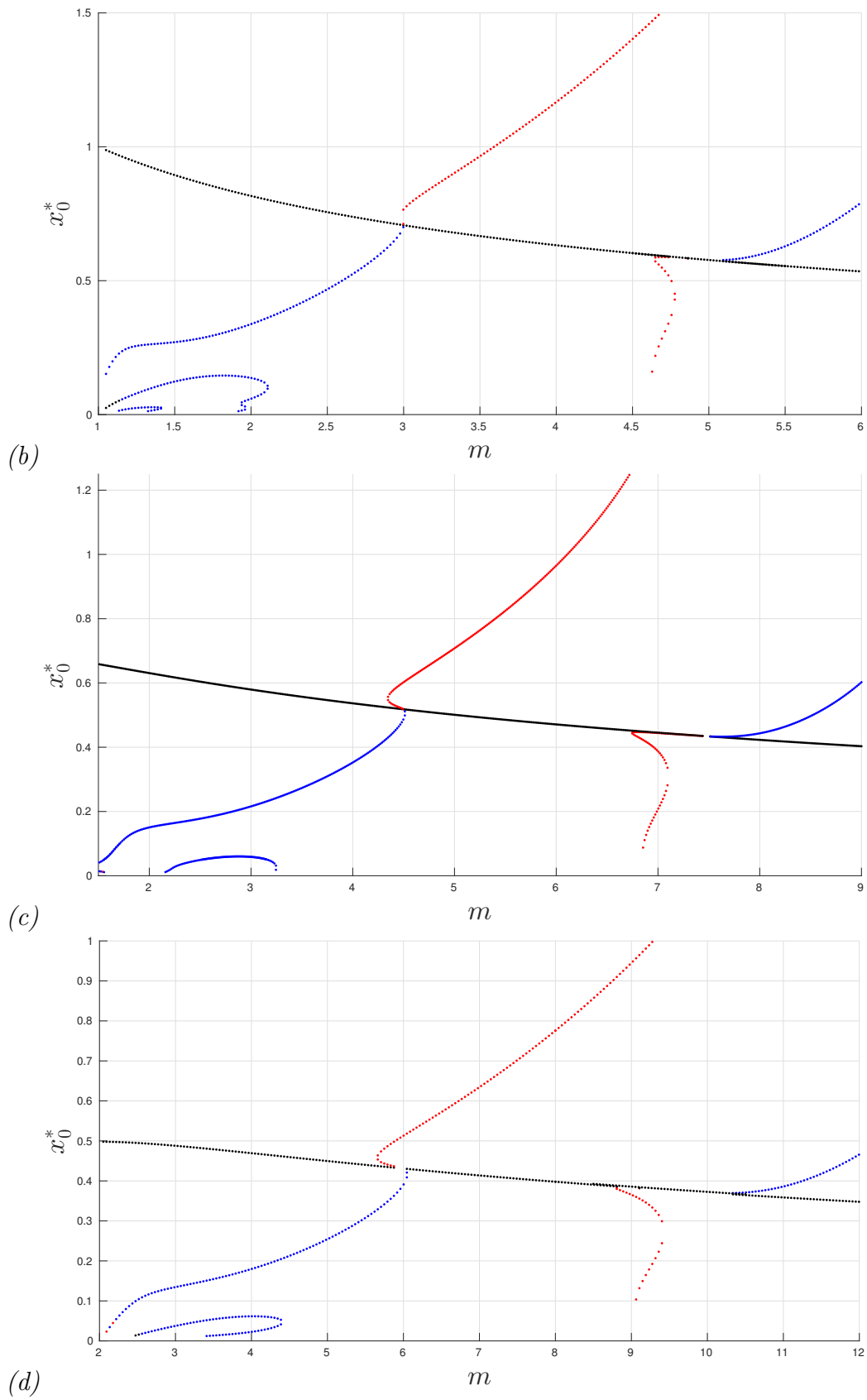


Figure 3.2

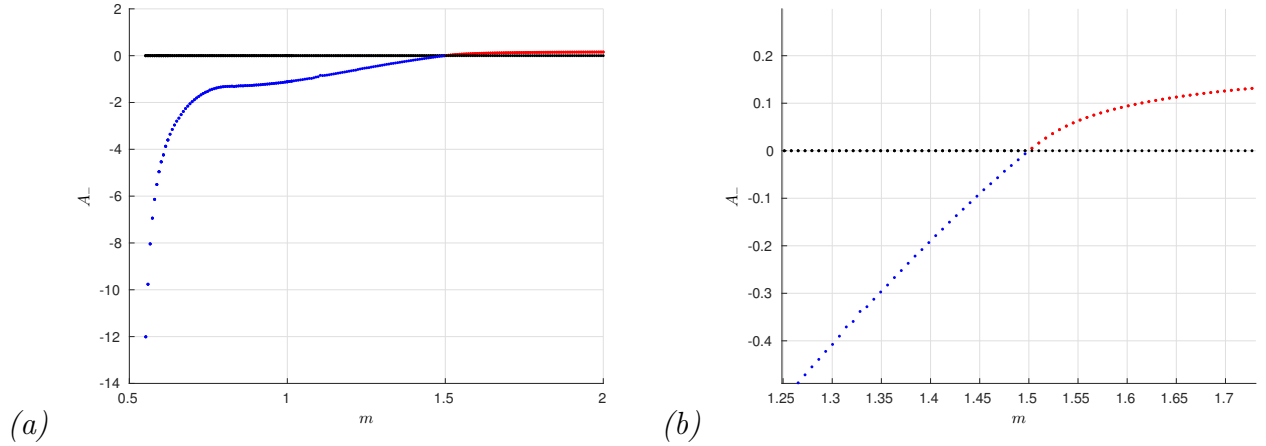


Figure 3.3: Panel (a) shows the variation of  $A_-$  with  $m$  along the red and blue curves emanating from the black curve near  $m = \frac{3}{2}$  with  $n = \frac{1}{2}$ . Panel (b) shows the same plot zoomed in to see positive values of  $A_-$ .

### 3.2 $H_+(t > 0)$

Solutions to (1.3) for time after reversing can be constructed with a numerical routine similar to that described in (3.1). In this case trajectories can be constructed from small to infinite values of  $H_+$ . This can be done by integrating the system (2.1) from the near-field equilibrium point  $(A_+, 0, 0)$  towards the far-field equilibrium point  $(x_0, 0, 0)$ . This done with the following numerical routine:

1. Select a value of  $A_+ \neq 0$ . Since this is an equilibrium point the initial conditions a small step  $\epsilon \ll 1$  away must be used. For  $A_+ > 0$  the trajectory will follow the center manifold (2.2). Taking the step  $\epsilon$  in the  $\xi$  direction the initial values for  $u$  and  $w$  are determined from the asymptotic behaviour:

$$\begin{cases} \xi = A_+ + \epsilon, \\ u = \left(\frac{2}{m+1-n}\right) \left(\frac{\epsilon}{A_+}\right)^{\frac{1}{1-n}}, \\ w = \left(\frac{2(1-n)}{(m+1-n)A_+}\right) \left(\frac{2\epsilon}{(m+1-n)A_+}\right)^{\frac{m+n}{1-n}}. \end{cases}$$

For  $A_+ < 0$  the trajectory will be along the unstable manifold (2.3) and the initial values of  $u$  and  $w$  are determined from the asymptotic behaviour:

$$\begin{cases} \xi = A_+ + \epsilon, \\ u = \left( \frac{m(m+1-n)|A_+|\epsilon}{2(1-n)} \right)^{\frac{1}{m}}, \\ w = \left( \frac{2(1-n)}{(m+1-n)A_+} \right) \left( \frac{m(m+1-n)|A_+|\epsilon}{2(1-n)} \right)^{\frac{1}{m}}. \end{cases}$$

In either case the system can then be integrated with increasing values of  $\tau$ . This was carried out with the `ode45` routine in MATLAB with  $\epsilon = 10^{-1}$ .

2. All trajectories leaving the near field along the center or unstable manifold will eventually approach the equilibrium point  $(x_0, 0, 0)$  in the far-field. In this case rather than switching to the far-field system the value of  $x_0$  can be found to arbitrary accuracy simply through the value of  $\xi u^{-(m+1-n)/2} \approx x_0$  at some very large value of  $\tau = \tau_\infty$ . Here,  $\tau_\infty \sim 10^5$  was found to be sufficient.

Carrying this out for a variety of choices of  $A_+$  it appears that  $x_0$  is a monotonically increasing function of  $A_+$ . A plot for different values of  $m$  and  $n$  can be found in Figure 3.4.

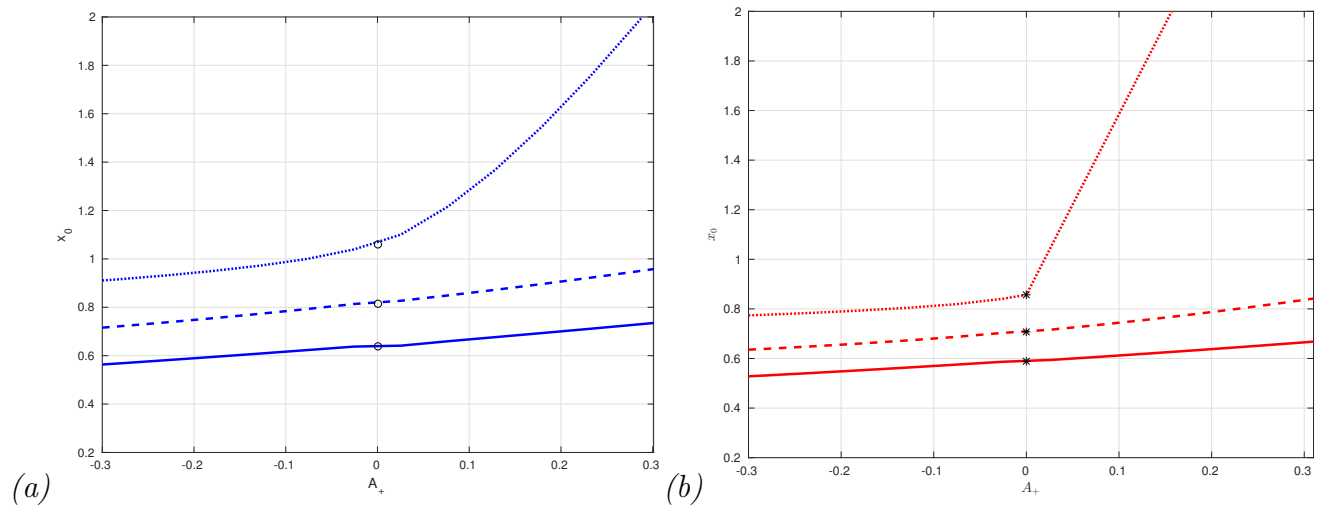


Figure 3.4: Plots of variation of  $x_0$  with  $A_+$  for different values of  $m$  and  $n$ : (a)  $m = 2$  and (b)  $m = 3$ . The solid, dashed and dotted lines correspond to  $n = -1/2$ ,  $n = 0$ , and  $n = +1/2$  respectively. The markers at  $A_+ = 0$  correspond to  $x_0 = x_Q$  for the stationary solution (1.9).

### 3.3 Summary

The main results are as follows: (i) for each value of  $m$  and  $n$  such that  $m > 0$ ,  $n < 1$ , and  $m + n > 1$ , there exists at least one value of  $x_0 = x_0^*$  (different from  $x_0 = x_Q$ ) that defines a trajectory emanating from  $(x, y, z) = (x_0^*, 0, 0)$  and terminating at  $(\xi, u, w) = (A_-, 0, 0)$

and thus is a suitable solution for  $H_-$ , and (ii) for every value of  $A_+ \in \mathbb{R}$  there exists a corresponding value of  $x_0$  and thus there are an infinite number of suitable solutions for  $H_+$ .

The remaining step in obtaining a physically relevant solution is then to invoke the condition (1.7) to match a particular  $H_+$  to the obtained  $H_-$ . This condition is equivalent to requiring that  $H_+$  and  $H_-$  have the same value of  $x_0$ . Any solution for  $H_-$  is characterized by a single value of  $x_0$  which then corresponds to a unique value of  $A_+$ .

## 4 Location of Bifurcations

As seen in Figure 3.2 the self-similar solutions bifurcate off of the stationary solution (1.9) where  $A = 0$ . The stationary solution is given again by:

$$H_0(\xi) = \left( \frac{\xi}{x_Q} \right)^{\frac{2}{m+1-n}}, \quad x_Q^2 = \frac{2(m+1+n)}{(m+1-n)^2}$$

Near the bifurcation, the new self-similar solution can be found to leading order by linearizing (1.3) with

$$H_-(\xi) = H_0(\xi) + v(\xi)$$

The allowed locations for bifurcation in the parameter space can be found by searching for the zero eigenvalue of the operator  $A$  in the linear eigenvalue problem

$$Av = \frac{d^2}{d\xi^2} (H_0^m v) - \frac{m+1-n}{2(1-n)} \xi \frac{dv}{d\xi} - nH_0^{n-1} v + \frac{1}{1-n} v = \lambda v .$$

Substituting the explicit form of  $H_0$  and changing variables to  $z = \frac{\xi}{x_Q}$  for neatness, this is equivalent to the eigenvalue problem for an operator  $B$  such that:

$$Bv = \frac{d^2}{dz^2} \left( z^{\frac{2m}{m+1-n}} v \right) - \frac{m+1-n}{2(1-n)} x_Q^2 z \frac{dv}{dz} - n x_Q^2 z^{\frac{2(1-n)}{m+1-n}} v = \mu v .$$

where  $\mu = x_Q^2(\lambda - \frac{1}{1-n})$ . Analysis is challenging due to the complicated form of the exponents but this equation can be greatly simplified with the change of variables:

$$y = \frac{m+1-n}{1-n} z^{\frac{1-n}{m+1-n}}$$

This results in another eigenvalue problem:

$$\frac{d^2 v}{dy^2} + \left( \frac{3m}{(1-n)y} - \frac{x_Q^2 y}{2} \right) \frac{dv}{dy} + \left( \frac{2(m^2 - m - n - n^2)}{(1-n)^2 y^2} \right) v = \mu v .$$

As  $y = 0$  is a regular singular point a Frobenius series solution can be obtained. Alternatively the terms with containing  $\frac{dv}{dy}$  can be removed with the transformation

$$w(y) = u(y)e^{\int \left( \frac{x_Q^2 y}{2} - \frac{3m}{2(1-n)y} \right) dy}$$

which results in the following eigenvalue problem

$$\frac{d^2 u}{dy^2} - \left( \frac{(m+4n)(m+2n+2)}{4(1-n)^2 y^2} + \frac{x_Q^4 y^2}{16} \right) u = \left( \mu - \frac{(3m+1-n)x_Q^2}{4(1-n)} \right) u .$$

This equation is in the same form as the Schrödinger equation for a 3-dimensional isotropic harmonic oscillator, i.e.

$$\frac{d^2 u}{dr^2} - \left( \frac{\ell(\ell+1)}{r^2} + \frac{M\omega^2 r^2}{2} \right) u = \frac{2ME}{\hbar^2} u$$

for a particle of mass  $M$  with energy  $E$ . This is a well-studied problem found in many textbooks [11]. The permissible energy values are

$$E_k = \left( 2k + \ell + \frac{3}{2} \right) \hbar\omega, \quad \text{with } k \in \mathbb{N} \quad \text{and} \quad \ell \in \{0, 1, \dots, k\} .$$

These correspond well to the eigenvalues for  $\lambda$  and  $\mu$  and thereby the following expressions can be found:

$$\mu - \frac{(3m+1-n)x_Q^2}{4(1-n)} = \frac{x_Q^2}{2} \left( 2k + \frac{m+4n}{2(1-n)} + \frac{3}{2} \right) ,$$

$$\lambda = \frac{m}{2} - (1-n)\left(k - \frac{1}{2}\right) .$$

The zero eigenvalue determines the values of  $m$  where a bifurcation can occur.

$$m = (1-n)(2k-1) \quad \text{for } k \in \mathbb{N} .$$

This is the main result, which corresponds well to the bifurcation values seen in Figure 3.2.

## 5 Conclusion

Self-similar reversing and anti-reversing solutions have been constructed for the nonlinear diffusion equation (1.1) with parameters  $m > 0$ ,  $n < 1$  and  $m+n > 1$ . These solutions were constructed using the dynamical systems framework of §2 which parametrizes trajectories in. The numerical routine described in §3 produces a matching pair of solutions  $H_-$  and  $H_+$

of the differential equations (1.3) which can then be transformed into physically meaningful solutions via the self-similar reduction (1.2). The appearance of these solutions at particular locations as branches off of the stationary solution (1.9) was justified in §4.

For every value of  $m$  and  $n$  within the constraints at least one suitable solution was identified. This solution is in addition to the exact solution (1.9) which in the original space and time variables does not exhibit reversing or anti-reversing behaviour. It was found that there are a limited number of  $H_-$  solutions, each of which is defined by a pair of values  $x_0^*$  and  $A_-$ . On the other hand, there are an infinite number of  $H_+$  solutions each corresponding to a pair of values  $x_0$  and  $A_+$ . A full solution then corresponds to one of the  $H_-$  solutions and the  $H_+$  solution with a matching  $x_0$  value. This determines a complete solution with reversing behaviour determined by the values of  $A_+$  and  $A_-$ . Solutions with  $A_-, A_+ > 0$  correspond to a reversing solution where the left interfaces advances for  $t < 0$  and then recedes for  $t > 0$ . Solutions with  $A_-, A_+ < 0$  correspond to an anti-reversing solution where the interface recedes for  $t < 0$  and then advances for  $t > 0$ .

The nonlinear diffusion admits two different traveling wave solutions, one with advancing interfaces driven by diffusion

$$h \sim (x - \ell(t))^{1/m}, \quad \dot{\ell}(t) < 0 ,$$

and the other with receding interfaces driven by absorption

$$h \sim (x - \ell(t))^{1/(1-n)}, \quad \dot{\ell}(t) > 0 .$$

This study describes the transition between the two behaviours. Any numerical scheme attempting to solve (1.1) must also capture this transition. In general 1.1 is hard to solve numerically because it has a free boundary, is nonlinear and is degenerate ( $h' = \infty$  at the interface). The results of this report are robust and therefore can be used to validate PDE methods to solve (1.1).

## References

- [1] J. M. Acton, H. E. Huppert and M. G. Worster, *Two dimensional viscous gravity currents flowing over a deep porous medium*, J. Fluid. Mech. 440 (2001), pp. 359-380.
- [2] D. G. Aronson, *Regularity properties of flows through porous media*, SIAM J. Appl. Math. 17 (1969), pp. 461-467.

- [3] J. M. Foster and D. E. Pelinovsky, *Self-similar solutions for reversing interfaces in the nonlinear diffusion equation with constant absorption*, arXiv:1506.05058v1 (2015)
- [4] J. M. Foster, C. P. Please, A. D. Fitt, and G. Richardson, *The reversing of interfaces in slow diffusion processes with strong absorption*, SIAM J. Appl. Math. 72 (2012), pp. 144-162
- [5] V. A. Galaktionov, S. I. Shmarev, and J. L. Vazquez, *Regularity of interfaces in diffusion processes under the influence of strong absorption*, Arch. Ration. Mech. Anal. 149 (1999), pp. 183-212
- [6] M. L. Gandarias, *Classical point symmetries of a porous medium equation*, J. Phys. A.: Math. Theor. 29 (1994), pp. 607-633.
- [7] M. E. Gurtin, *On the diffusion of biological populations*. Math. Biosci. 33 (1977), pp. 35-49.
- [8] M. A. Herrero and J. L. Vazquez, *The one-dimensional nonlinear heat equation with absorption: regularity of solutions and interfaces*, SIAM J. Math. Anal. 18 (1987), pp. 149-167
- [9] A. S. Kalashnikov, *The propagation of disturbances in problems of nonlinear heat conduction with absorption*, USSR Comput. Math. Phys. 14 (1974), pp. 70-85.
- [10] R. Kersner, *Nonlinear heat conduction with absorption: Space localization and extinction in finite time*, SIAM J. Appl. Math. Phys. 43 (1983), pp. 1274-1285.
- [11] L. D. Landau and E. M. Lifshitz, *Quantum Mechanics: Non-relativistic Theory*, 3rd ed. Pergamon Press (1977)